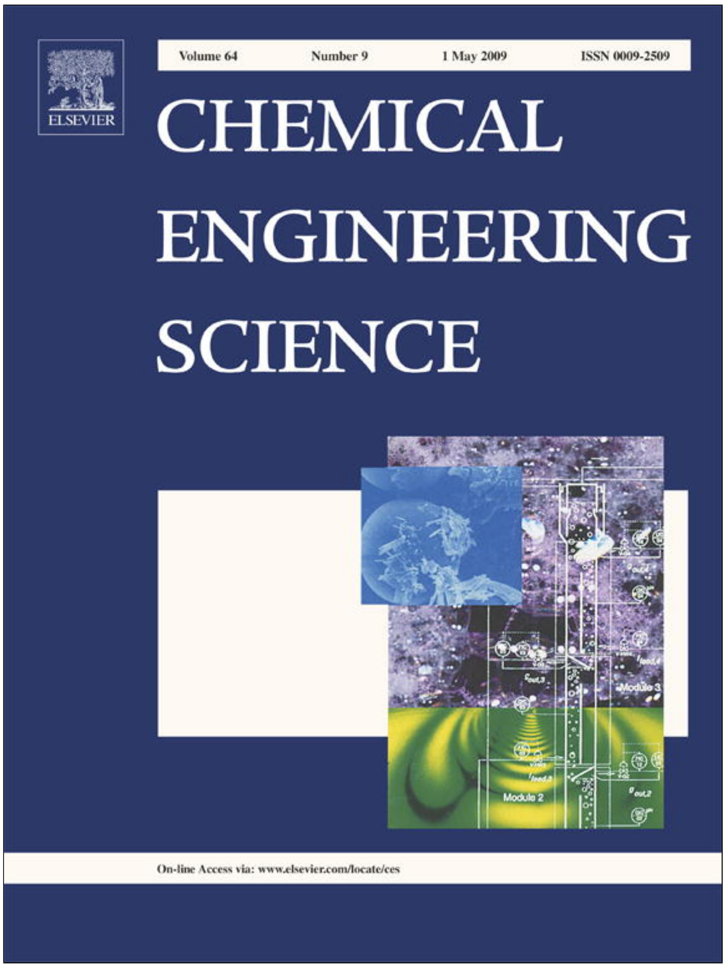

Volume 64 Number 9 1 May 2009 ISSN 0009-2509

ELSEVIER

CHEMICAL
ENGINEERING
SCIENCE

On-line Access via: www.elsevier.com/locate/ces

Chemical Engineering Science 64 (2009) 2226–2233

Contents lists available at ScienceDirect

Chemical Engineering Science

journal homepage: www.elsevier.com/locate/ces

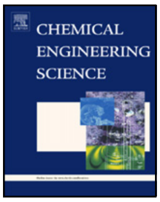

Structured chiral adsorbent formed by cyclodextrin modified layered solid film

Xiaolei Liu[a,b], Min Wei[a,*], David G. Evans[a], Xue Duan[a]

[a]State Key Laboratory of Chemical Resource Engineering, Beijing University of Chemical Technology, Beijing 100029, PR China
[b]Chemical Engineering Department, Zibo Vocational Institute, Zibo 255314, PR China

ARTICLE INFO

Article history:
Received 16 October 2008
Received in revised form 1 February 2009
Accepted 3 February 2009
Available online 12 February 2009

Keywords:
Layered double hydroxides
Composites
Film
Enantioselective
Adsorption
Nanostructure

ABSTRACT

The film of carboxymethyl-β-cyclodextrin-intercalated Zn–Al layered double hydroxide (CMCD-LDH) has been prepared by in situ crystallization on a porous anodic alumina/aluminum (PAO/Al) substrate. This film can be used to enantioselectively separate racemic molecules, 1-phenyl-1,2-ethanediol (PED). The adsorption isotherms of enantioselective as well as non-enantioselective adsorption of PED by CMCD-LDH film have been investigated, and it was found that the Langmuir–Freundlich and Freundlich model can be, respectively, used to describe the two different adsorptions satisfactorily. Furthermore, the plane sheet diffusion model was successfully validated in this work. Diffusivities (D) of PED in CMCD-LDH film were determined from the Fickian diffusion model at various temperatures. As the structured CMCD-LDH film is conveniently used and exhibits high enantioselective adsorption ratio, it can be expected that this film could be feasibly applied in the field of industrial chiral adsorption and separation.

1. Introduction

The enantioselective separation of chiral molecules by cyclodextrins (CDs) and chemically modified CDs is an important aspect of analytical and pharmaceutical research and has been the subject with growing interest both experimentally and theoretically (Lipkowitz et al., 1997; Rekharsky and Inoue, 2002; Xiao et al., 2007; Xu and McCarroll, 2005). CDs are cyclic (α-1,4)-linked oligosaccharides composed of α-D-glucopiranose. They are truncated cone-shaped molecules with a hydrophilic outside and a hydrophobic hollow (Faucci et al., 2002; Szejtli, 1998), as a result, CDs can form inclusion complexes with various organic molecules. Since they are derived from glucose units, the CDs molecules are inherently dissymmetric and are thus able to distinguish between stereochemical isomers including enantiomers. The versatility of these macrocycles is remarkable, and they are extensively used in chiral chromatography due to their price-to-performance ratio. Both native and derivative CDs have been used to separate enantiomers in planar chromatography (TLC) (Sherma, 2002), high-performance liquid chromatography (HPLC) (Sun et al., 2007), super and subcritical fluid-phase chromatography, and more recently, they were used as additives that enantioselectively bind and control the migratory aptitudes of analytes in capillary electrophoresis (Nishi and Terabe, 1995).

Layered double hydroxides (LDHs, also known as anionic clays), are a class of layered materials consisting of positively charged brucite-like layers and exchangeable interlayer anions, which have recently received increasing attention, owing to their versatility and usefulness in a wide range of technological applications such as catalysis (Sels et al., 2005; Wei et al., 2007), functional materials (Hou and Kirkpatrick, 2002; Williams et al., 2006; Xu and Braterman, 2007; Zou et al., 2007), two-dimensional solid-state nanoreactors (Gerardin et al., 2005), bioactive nanocomposites (Choy et al., 2000), and so on. LDHs can be represented by the general formula $[\mathrm{M}^{2+}_{1-x}\mathrm{M}^{3+}_{x}(\mathrm{OH})_2]^{x+}(\mathrm{An}^{-}_{x/n})\cdot m\mathrm{H_2O}$, where M^{2+} and M^{3+} are divalent and trivalent metal cations, such as Mg^{2+} and Al^{3+}, respectively, and A^{n-} is an anion, such as $\mathrm{CO_3}^{2-}$, $\mathrm{SO_4}^{2-}$, or $\mathrm{NO_3}^{-}$. The structure of LDHs is most clearly described by considering the brucite-like structure, $\mathrm{M(OH)_2}$, which consists of M^{2+} ions coordinated octahedrally by hydroxyl groups, with the octahedral units sharing edges to form infinite, charge-neutral layers. In an LDHs material, isomorphous replacement of a fraction of the divalent cations with a trivalent cation occurs and generates a positive charge on the layers, which necessitates the presence of interlayer charge-balancing anions. In the commonly observed powder form, LDHs have a house-of-cards structure involving edge-to-face particle interactions, which limits their research and application (Gursky et al., 2006). The most effective solution to this problem may be preparation of LDHs film on substrates (Chen et al., 2006; Gardner et al., 2001; Lee et al., 2004, 2006; Li et al., 2007; Liu et al., 2006; Lü et al., 2007). Gardner et al. (2001) found that the colloidal LDH suspensions obtained by hydrolysis of alkoxide-intercalated LDH derivatives were able to form transparent film. Lee and co-workers (2004, 2006) used the ultrasonification method to prepare monolayer of LDH films with a high packing density and a preferred orientation with the c-axis perpendicular to

---

[*] Corresponding author. Tel.: +86 10 64412131; fax: +86 10 64425385.
E-mail address: weimin@mail.buct.edu.cn (M. Wei).

0009-2509/$ - see front matter © 2009 Elsevier Ltd. All rights reserved.
doi:10.1016/j.ces.2009.02.007

the substrate surface, whilst Liu (2006) and Li (2007) reported that the exfoliation of LDH in organic solvents (formamide, for instance) gives colloidal LDH particles which can be used as building blocks in the preparation of transparent oriented LDH films by layer-by-layer techniques. Our group has recently reported fabrication of NiAl-LDH film with the *c*-axis parallel to the substrate, by means of employing porous anodic alumina/aluminum (PAO/Al) as both substrate and sole source of aluminum (Chen et al., 2006).

In recent years, the immobilization of CDs with layered supports has attracted much attention. Modified CDs have been used as a "guest" molecule incorporating into layered hosts such as α-zirconium phosphate (Kijima and Matsui, 1986), montmorillonite (Kijima et al., 1984), and LDHs (Zhao and Vance, 1997; Mohanambe and Vasudevan, 2005). In our previous work, the intercalation of sulfated β-CD into LDH as well as the structural characterization, thermal decomposition behavior have been studied (Wang et al., 2004; Wei et al., 2005). Recently we have shown that when the internal surfaces of the layered anionic clay (Zn–Al LDH) are functionalized by anchoring anionic carboxymethyl β-cyclodextrin (CMCD) cavities, neutral racemic guest molecule, 1-phenyl-1,2-ethanediol (PED), can be enantioselectively included within it (Liu et al., 2007). Furthermore, the adsorption isotherms of enantioselective and non-enantioselective adsorption of PED by CMCD-LDH have been studied by using a batch method. The parallel diffusion model is successfully used in this adsorption process.

However, it was found in our previous work that the enantioselective adsorption ratio of CMCD-LDH powder is not high (the maximum is less than 40%). The reason for this is that a large amount of non-enantioselective adsorption by external surface of LDH powder occurs. In order to improve the enantioselective adsorption ratio and thus enhance the chiral separation, it is necessary to decrease the ratio of external surface of LDH. From this point of view, in this study, the structured CMCD-LDH film was fabricated by the method of *in situ* crystallization on a PAO/Al substrate. In this film, the *ab*-face of LDH microcrystals is perpendicular to the substrate, and the edges of LDH plates are exposed to the outside, which is favorable to adsorb solute from solutions. Furthermore, the immobilized LDH nanocrystals film can be conveniently used for manipulation as structured adsorbents. In order to study the properties of enantioselective adsorption of the CMCD-LDH film, we chose racemic PED as the model molecule, for optically active PED is a valuable and versatile chiral building block for the synthesis of pharmaceuticals, agrochemicals, pheromones and liquid crystals. Of the racemate, (*S*)-enantiomer can be further used as precursor for the production of chiral biphosphines and chiral initiator for stereoselective polymerization (Iwasaki et al., 1999). The adsorption isotherms of enantioselective as well as non-enantioselective adsorption of PED by CMCD-LDH film have been studied by using a batch method. Furthermore, the plane sheet diffusion model was successfully validated in this work. Diffusivities (D) of PED in CMCD-LDH film were determined from the Fickian diffusion model at various temperatures. Compared with the chiral adsorption by CMCD-LDH powder sample in our previous study (Liu et al., 2007), the structured CMCD-LDH adsorbent film is more conveniently used and shows higher enantioselective adsorption ratio. Therefore, a novel and simple method to fabricate a CD modified LDH film has been developed in this work, and its chiral adsorption properties for racemic PED were demonstrated. It can be expected that this structured film could be feasibly applied as the basis of a novel chiral separation system.

2. Experimental section

2.1. Reagents

All chemicals including $Zn(NO_3)_2 \cdot 6H_2O$, NH_4NO_3, $NH_3 \cdot H_2O$, chloroactic acid, β-CD and (*R*, *S*)-PED were of analytical grade. β-CD was purchased from Aldrich, and the others from the Beijing Chemical Plant Limited. Aluminum metal sheet was purchased from Shanghai Jing Xi Chemical Technology Co., Ltd., purity: $>99.5\%$, thickness: 0.1 mm.

2.2. Preparation and characterization

2.2.1. Synthesis of CMCD (4.1)

CMCD was synthesized according to the procedure described in the literature (Park et al., 2001) with some modifications. In brief, CD (32.4 g) and NaOH (35.2 g) was dissolved in 200 ml of water, and monochloroacetic acid (37.8 g) was added with gentle stirring. The mixture was heated at 80 °C for 3 h. The solution was then cooled in an ice bath and the pH was adjusted to 6.0 with concentrated hydrochloric acid. Methanol was gradually added into the solution with stirring to obtain CMCD precipitation. The average number of carboxylate groups (4.1) per CMCD was calculated using ^{1}H NMR (Ravoo et al., 2001).

2.2.2. Synthesis of CMCD-LDH film

The CMCD-LDH film was prepared by a novel and simple strategy, i.e., *in situ* crystallization on a PAO/Al substrate. The PAO film was fabricated by anodizing an aluminum metal sheet for 50 min in a thermostatic bath of 1 M H_2SO_4 at a temperature of 25 °C and with a current density of 20 mA/cm^2 (Chen et al., 2006). In this experiment, PAO/Al was used as both the substrate and the sole source of aluminum, and the CMCD-LDH film was prepared by one-step synthesis method with easy manipulation. In a typical procedure, 0.01 mol of $Zn(NO_3)_2 \cdot 6H_2O$, 0.06 mol of NH_4NO_3, and 0.001 mol of CMCD were dissolved in deionized water to form a clear solution with a total volume of 100 ml, and the pH was adjusted to 6.5 by adding diluted ammonia (1% NH_4OH). The PAO/Al substrate was then placed vertically in the solution at 70 °C for 48 h, to obtain the CMCD-LDH microcrystals grown on the surface of the substrate. Finally, the substrate was taken out, rinsed with water, and dried at room temperature. Based on the difference between the initial and final mass of the substrate, the weight of CMCD-LDH film per unit area of the substrate was calculated to be 2.80×10^{-2} kg/m^2.

2.2.3. Adsorption experiments

PED sorption experiments were carried out using a batch method. Both the effects of contact time and PED concentration on the adsorption were investigated, and the effect of contact time was used to determine kinetic model of PED sorption and equilibrium time. A series of 1.5×10^{-5} m^3 of PED solution (typically ranging from 0.0 to 96.6 mol/m^3) were added to beakers, and the structured CMCD-LDH film (with the area of 9×10^{-4} m^2) was immersed into the solution (as shown in Fig. 1). The beakers were placed in a water bath at certain temperature (e.g. 303 K) and gently shaken for specific time period to reach adsorption equilibrium. The PED concentration was determined using UV–vis spectrophotometer at $\lambda = 256$ nm. The amount of PED adsorbed by the CMCD-LDH film was calculated by the difference between the initial (C_0) and equilibrium concentrations (C_e), per kg of LDHs adsorbent: $Q_e = (C_0 - C_e)\times V/m$.

2.2.4. Characterization

Powder X-ray diffraction (XRD) patterns of the samples were recorded using a Shimadzu XRD-6000 diffractometer with Cu-Kα radiation ($\lambda = 1.5406$ Å). The operating voltage and current were 40 kV and 30 mA, respectively. The step used was 0.02° s^{-1} in the 2θ range from 2° to 70°. The morphology of the CMCD-LDH film was investigated by using a scanning electron microscope (SEM) with an energy dispersive X-ray (EDX) attachment (SEM: Hitachi S-4700, EDX: Genesis 60). Fourier transform infrared (FT-IR) spectra were recorded using a Bruker Vector22 spectrophotometer in

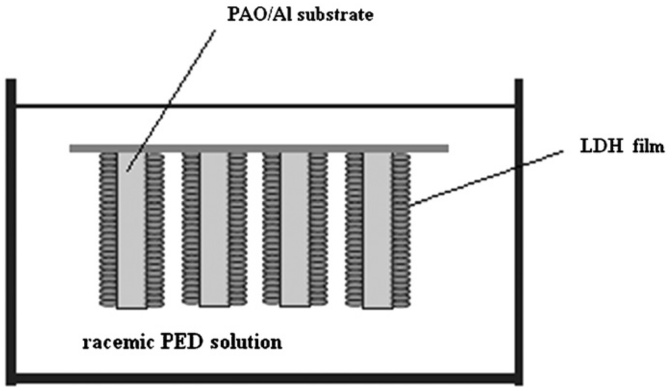

Fig. 1. Schematic representation for the adsorption of racemic PED by CMCD-LDH film.

the range 4000–400 cm^{-1} with 2 cm^{-1} resolution. The standard KBr disk method (1 mg of sample in 100 mg of KBr) was used. An UV–vis spectrophotometer (Shimadzu UV-2501PC) was employed to measure the absorbance spectra of compounds in the 200–700 nm wavelength range. The concentration of PED in the solutions, before and after adsorption experiments, was determined by the UV–vis spectra at the wavelength of 256 nm. Chiral HPLC (daicel chiralcel OB-H, 5% *i*PrOH in hexane, flow rate 0.5 ml/min) was used to determine e.e.% of the solutions after the adsorption experiment.

3. Experimental results

3.1. Characterization of CMCD-LDH film

3.1.1. X-ray diffraction

The CMCD intercalated LDH film (CMCD-LDH film) was synthesized by *in situ* crystallization on PAO/Al substrate as described in the experimental part. Fig. 2 illustrates the XRD patterns of the CMCD-LDH film as well as the PAO/Al substrate. The sequence of strong (0 0 3), (0 0 6) reflections at low angle and the (0 1 2) reflection at high angle for the film (Fig. 2b) indicates formation of well-crystallized hydrotalcite-like LDH phase. The reflection can be indexed to a hexagonal lattice with *R*-3m rhombohedral symmetry, commonly used for the description of LDH structures. The interlayer distance of CMCD-LDH is 1.855 nm, which is slightly larger than that of the CMCD-LDH powder (Liu et al., 2007). Since the thickness of the LDH hydroxide basal layer is 0.480 nm, the gallery height is 1.375 nm. CD should be regarded as truncated cone rather than a cylinder. There are seven primary and fourteen secondary hydroxyl groups along the β-CD cavity, which has an approximate torus thickness of 0.78 nm, an outer diameter of 1.53 nm and an inner diameter of 0.78 nm (Szejtli, 1998). Taking into account the dimensions of the β-CD molecule and the rule of charge balance, the CMCD (4.1) anions can only adopt a monolayer arrangement with their cavities axis perpendicular to the LDH layer and carboxymethyl groups on adjacent CD molecules attached alternately to the upper and lower LDH layer surfaces. This is similar to the arrangement in our previous research of CMCD-LDH powder (Liu et al., 2007).

3.1.2. Infrared spectroscopy

The FT-IR spectra of CMCD and the CMCD-LDH powder scraped from the film are shown in Fig. 3. In the infrared spectrum of the as-synthesized sodium salt of CMCD, a broad strong absorption band at 3405 cm^{-1} is observed, which can be attributed to OH combination stretching vibrations of hydroxyl groups and physically adsorbed water. An absorption at 2929 cm^{-1} is due to the stretching vibration of –CH$_2$. Two strong bands at 1606 and 1423 cm^{-1} are attributed to the asymmetric and symmetric stretching vibrations of carboxylate –COO$^-$, respectively. Bands at 1161 and 1034 cm^{-1} are assigned to absorption of C–O, C–O–C of glucose units. In the case of the CMCD-LDH powder scraped from the film, most bands of CMCD show no obvious change upon intercalation into LDH (Fig. 3b). The asymmetric stretching band of –COO$^-$ moves slightly toward to low frequency, at 1593 cm^{-1}. This spectral change may be related to the formation of hydrogen bonding between the carboxylate and the hydroxyl in LDH layer. Moreover, the metal–hydroxyl (M–OH) stretching modes of LDH layer appear at 426 cm^{-1}.

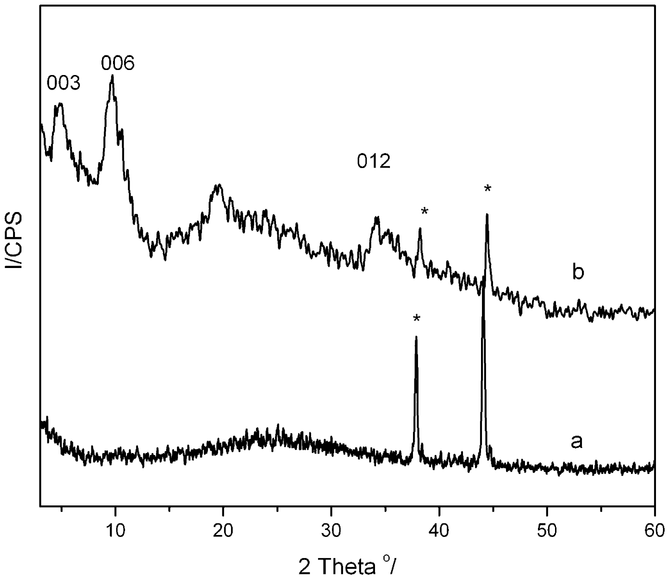

Fig. 2. XRD patterns of: (a) the PAO/Al substrate and (b) the CMCD-LDH film. Asterisk denotes the reflections of Al substrate.

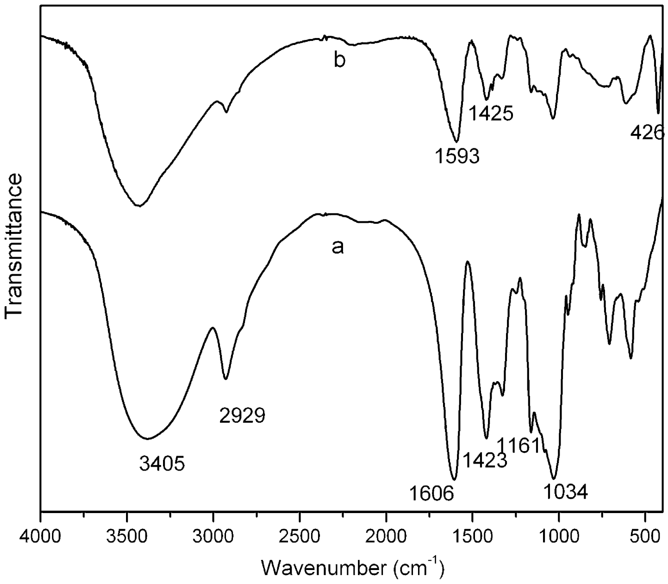

Fig. 3. FT-IR spectra of: (a) CMCD and (b) the CMCD-LDH powder scraped from the film.

3.1.3. SEM and EDX

The morphology of the PAO/Al substrate and CMCD-LDH film was studied by SEM. The top surface (Fig. 4a) of PAO/Al substrate shows

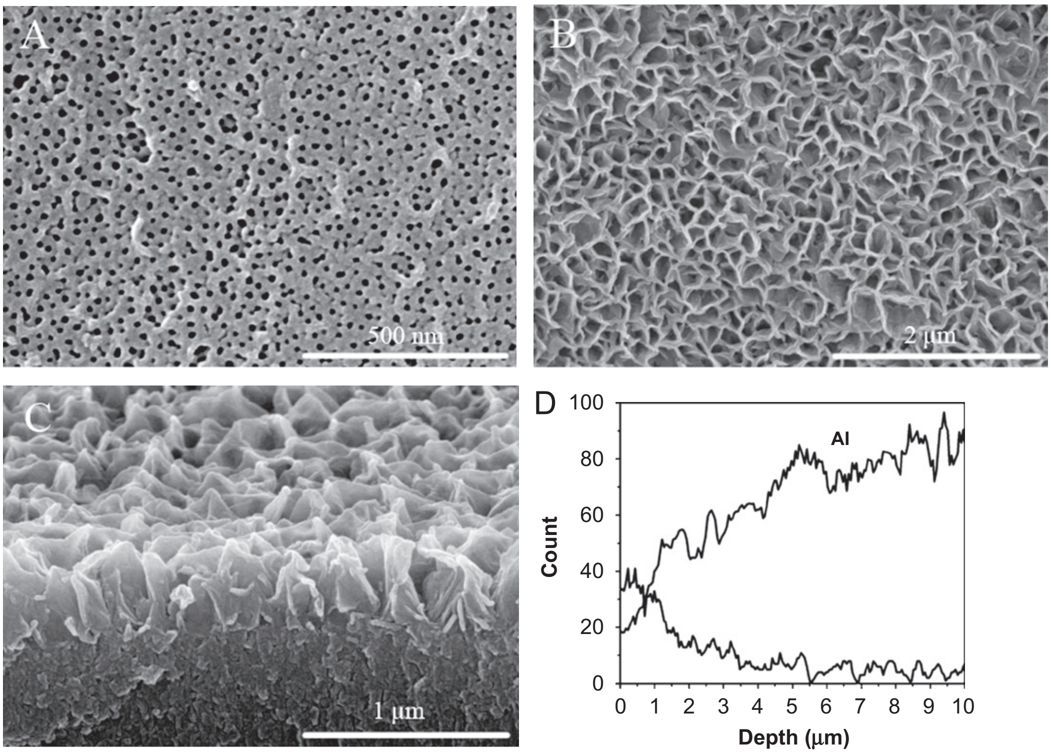

Fig. 4. SEM images of: (A) the PAO/Al substrate, (B) surface-view of the CMCD-LDH film on PAO/Al substrate, (C) edge-view of the CMCD-LDH film, and (D) the energy dispersive X-ray line scan of the edge-view of the film.

that the PAO film has porous structure with pore diameter of ca. 20 nm. Fig. 4b exhibits the surface-view of the CMCD-LDH film after crystallization on the PAO/Al substrate at 70 °C for 48 h. The curved hexagonal faces of the LDH microcrystal can be clearly observed perpendicular to the substrate over the entire substrate surface. The edge-view of the CMCD-LDH film (Fig. 4c) demonstrates that only a monolayer of the LDH crystals with a thickness of ca. 0.5 μm was assembled on the PAO/Al substrate. These images indicate that the *ab*-face of LDH microcrystals is predominantly perpendicular with respect to the substrate. This observation can be confirmed by EDX analysis, displayed in Fig. 4d. The Zn/Al distribution ranges from 1.3 to 2.0 along EDX line scanning over the LDH film and a part of the PAO/Al substrate. At depths below 500 nm, however, the Zn profile of the EDX rapidly decreases to almost zero, indicating the absence of the Zn species inside the substrate.

3.2. Adsorption equilibrium

Chiral HPLC (daicel chiralcel OB–H, 5% *i*-PrOH in hexane, flow rate 0.5 ml/min) was used to determine e.e.% of the PED solution after the adsorption experiment. The results indicate that *R*-PED was adsorbed preferentially by CMCD-LDH film. It can be speculated that the adsorption of PED by CMCD-LDH film includes two parts: the enantioselective adsorption (Q_s) resulting from the chiral reorganization of interlayer immobilized CMCD and the non-enantioselective adsorption (Q_{non-s}) produced by the external surface of LDH, which can be calculated by

$$Q_s = C_t \times V \times e.e.\%/m \qquad (1)$$

$$Q_{non-s} = \frac{(C_0 - C_t) \times V - C_t \times V \times e.e.\%}{m} \qquad (2)$$

Thus the adsorption isotherms, including enantioselective and non-enantioselective adsorption, were plotted and shown in Fig. 5.

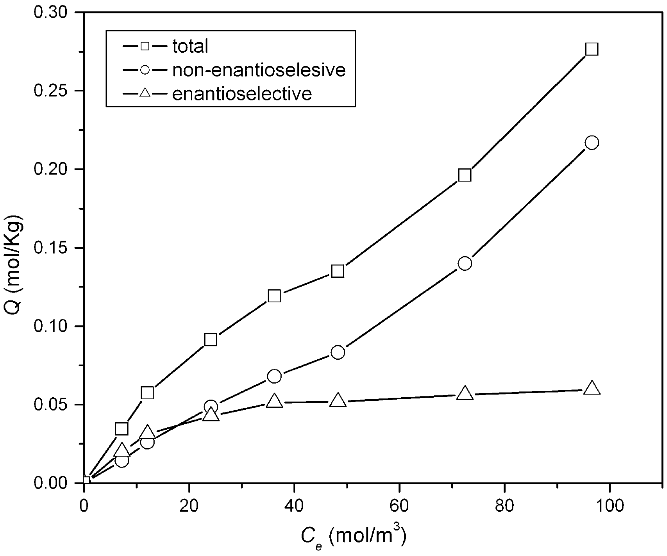

Fig. 5. The total, enantioselective, and non-enantioselective adsorption isotherms of PED by CMCD-LDH film at 323 K.

The total and non-enantioselective adsorption increase with the increase in concentration of PED, while the enantioselective adsorption by CMCD cavities has a maximum adsorption capacity.

The enantioselective adsorption data were modeled using two competitive adsorption-isotherm models: the Langmuir and the Langmuir–Freundlich (L–F).

(1) *Langmuir isotherm.* This isotherm model is widely used for physical adsorption from either gas or liquid solution. The

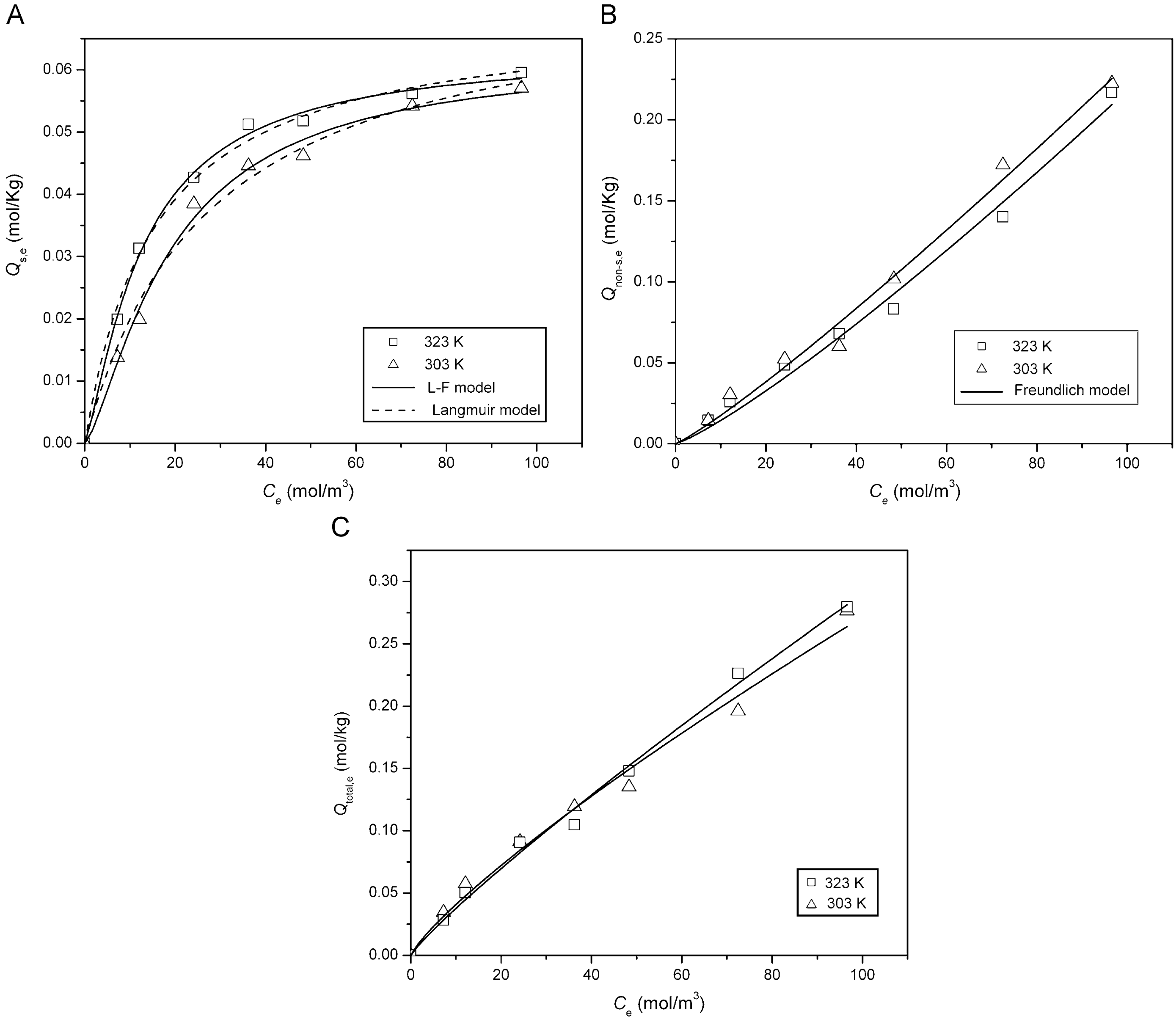

Fig. 6. (A) The enantioselective adsorption isotherms of *R*-PED by CMCD-LDH film fitted by Langmuir and L–F model, (B) the non-enantioselective adsorption, and (C) the total adsorption isotherms of (*R*, *S*)-PED by CMCD-LDH film fitted by Freundlich model at 303 and 323 K, respectively.

mathematical form of Langmuir model is

$$\frac{Q_e}{Q_m} = \frac{K_L C_e}{1 + K_L C_e} \tag{3}$$

where Q_e is the adsorbed amount, C_e the equilibrium concentration, and Q_m and K_L are isotherm parameters.

(2) L–F *isotherm.* The L–F isotherm (Eq. (4)), also known as the Sips equation (Sips, 1948), is a function that describes a specific relationship between the equilibrium concentration of bound and free guest in heterogeneous systems with three fitting coefficients: Q_m, K_L, and n. These coefficients have physical meaning: Q_m is the total number of binding sites; the variable K_L is related to the median binding affinity; n is the heterogeneity index, which varies from 0 to 1. For a homogeneous material, $n = 1$. When $n < 1$, the material is heterogeneous.

$$\frac{Q_e}{Q_m} = \frac{K_L C_e^n}{1 + K_L C_e^n} \tag{4}$$

According to the classification of Giles et al. (1960), although the enantioselective adsorption of PED by CMCD-LDH film has a maximum adsorption capacity, the shape of its isotherm cannot be considered simply as pure L-type. Fig. 6a displays the enantioselective adsorption isotherms of PED by CMCD-LDH film at different temperatures, fitted by Langmuir and L–F model, respectively. The experimental conditions, the estimated model parameters and regression coefficients (R^2) are reported in Table 1 for all enantioselective adsorption experimental runs.

As can be seen from Table 1, the regress coefficients (R^2) for the L–F model are larger than that of Langmuir model, and the experimental $Q_{s,e}$ values agree well with the calculated ones obtained from L–F model. This indicates that the L–F model can be used to describe the enantioselective adsorption of PED by CMCD-LDH film satisfactorily. Furthermore, it was found that the amount of enantioselective adsorption increases with the increase of temperature. The explanation for this behavior is straightforward. The

Table 1
Langmuir and L–F constants for the enantioelective adsorption of *R*-PED by CMCD-LDH film at different temperatures.

Temperature (K)	Langmuir model			L–F model			
	K_L (m^3/kg)	Q_m (mol/kg)	R^2	K_L (m^3/kg)	Q_m (mol/kg)	n	R^2
303	3.61×10^{-2}	7.44×10^{-2}	0.981	1.74×10^{-2}	6.25×10^{-2}	1.37	0.990
323	3.55×10^{-2}	7.56×10^{-2}	0.982	3.97×10^{-2}	6.32×10^{-2}	1.26	0.994

Table 2
Freundlich constants for the non-enantioselective and total adsorption of (*R*, *S*)-PED by CMCD-LDH film at different temperatures.

Temperature (K)	Non-enantioselective			Total		
	K	n	R^2	K	n	R^2
303	1.32×10^{-3}	0.889	0.989	6.13×10^{-3}	1.21	0.984
323	9.60×10^{-4}	0.848	0.988	4.88×10^{-3}	1.12	0.993

enantioselective adsorption is caused by the chiral inclusion of CD accommodated in the interlayer region of LDH, which is an energy-needed
process.

Fig. 6b and c display the non-enantioselective and total adsorption isotherms at 303 and 323 K, respectively. Owing to the shape of the isotherms, the non-enantioselective and total sorption data were analyzed based on Freundlich equation (Agrawal et al., 2004):

$$Q_e = KC_e^{1/n} \tag{5}$$

where Q_e is the amount of PED per unit weight of the LDH; C_e is the equilibrium concentration of PED in the solution (mol/m^3); K and n are Freundlich temperature-dependent constants. Table 2 lists the Freundlich constants for the non-enantioselective and total adsorption at different temperatures. The experimental $Q_{non-s,e}$ and $Q_{total,e}$ values are in high accordance with the calculated ones obtained from Freundlich model, indicating that both the non-enantioselective and total adsorption isotherms can be represented by the Freundlich model. As the non-enantioselective adsorption falls into physical adsorption by the external surface of LDH, the adsorption amount decreases with increasing temperature.

3.3. Study on the diffusion kinetics

Experimental data are fitted with an appropriate model in order to determine the value of the diffusion coefficient. Under the working conditions performed in the present experiments, mass-transfer phenomena can be described by Fick's law of diffusion. With the film thickness being low compared with its diameter, the CMCD-LDH film can be considered as a monodimensional slab and the equation describing one component diffusion in a nonstationary monodimensional homogeneous system (Crank, 1975) can be used, where D is the diffusion coefficient:

$$\frac{\partial C}{\partial t} = D\frac{\partial^2 C}{\partial x^2} \tag{6}$$

In this experiment, the CMCD-LDH film was immersed in a large volume of solution so that the amount of PED taken up by the film is a negligible fraction of the whole; the solution is well stirred, so the concentration of the solution remains constant. Taking into account the substrate of thickness a and the case of the diffusion through a plane sheet of thickness l, the boundary conditions can be written:

$$t = 0 \quad -l-a/2 < x < -a/2 \text{ and } a/2 < x < a/2 + l \quad C = 0 \tag{7}$$

$$t \geqslant 0 \quad x = -l - a/2 \quad C = C_0 \tag{8}$$

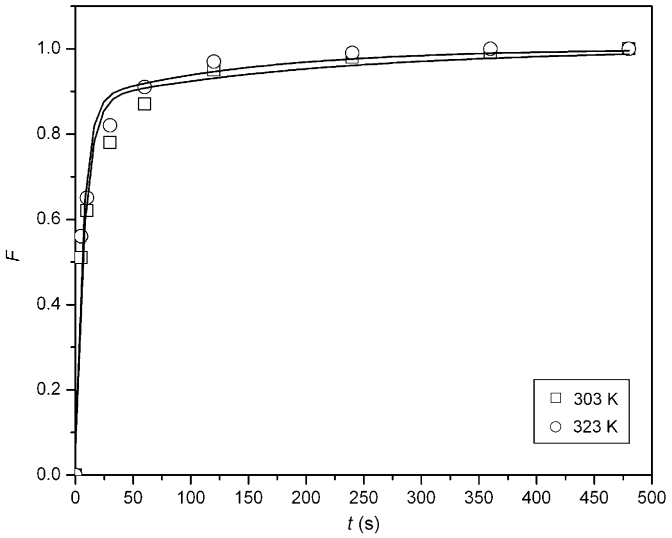

Fig. 7. Sorption kinetic curves of the PED by the CMCD-LDH film with $C_0 = 12.0\,\text{mol/m}^3$.

$$t \geqslant 0 \quad x = l + a/2 \quad C = C_0 \tag{9}$$

Solving Eq. (6) with the conditions of Eqs. (7)–(9) gives the concentration profile C inside the film; the total mass balance to the plane sheet then gives (Crank, 1975)

$$F = \frac{Q_t}{Q_e} = 1 - \frac{8}{\pi^2}\sum_{n=0}^{\infty}\frac{1}{(2n+1)^2}\exp\{-D(2n+1)^2\pi^2 t/4l^2\} \tag{10}$$

Initializing different values of D until the best fit was obtained. As shown in Fig. 7, the experimental values were well correlated by Eq. (10). The experimental values of D are 5.11×10^{-14} m^2/s at 303 K and 6.06×10^{-14} m^2/s at 323 K, respectively.

3.4. Comparison study on the adsorption of PED between CMCD-LDH film and powder

As discussed above, the structured CMCD-LDH film can be used to enantioselectively adsorb racemic PED. In accordance with the powder sample in our previous work (Liu et al., 2007), the enantioselective adsorption capacity of CMCD-LDH film is related to the interlayer CMCD molecules, while the non-enantioselective adsorption is produced by the multilayer adsorption of PED by the external surface of LDH. It was found that the L–F and Freundlich model could be respectively used to describe the two kinds of adsorptions satisfactorily, which is similar to the powder sample. However, due to the orientation of the CMCD-LDH microcrystals in the structured film, both the enantioselective adsorption ratio and sorption kinetics show differences from those of its powder sample. First of all, it can be seen that the enantioselective adsorption ratio of CMCD-LDH film is above 50% (Fig. 5) with low PED concentrations (0–20 mol/m^3), which is significantly higher than that of CMCD-LDH powder (the highest enantioselective adsorption ratio of CMCD-LDH powder is less than 40%). Secondly, the effective diffusivity of PED in the film is lower than that of the powder sample. These might be related to the reason that the CMCD-LDH film has lower external surface ratio compared with its powder form, which reduces the amount of non-enantioselective adsorption and also decelerates the adsorption process. As the structured CMCD-LDH film is conveniently used and exhibits higher enantioselective adsorption ratio, it can be expected that this structured film has prospective application in the field of enantioselective adsorption and separation.

4. Conclusions

We have demonstrated a facile method for the preparation of oriented CMCD-LDH film with curved hexagonal microstructure on a PAO/Al substrate. The as-prepared CMCD-LDH film shows excellent enantioselective adsorption for (*R*, *S*)-1-phenyl-1,2-ethanediol. The adsorption isotherms of enantioselective as well as non-enantioselective adsorption of PED by CMCD-LDH film have been investigated, and it was found that the Langmuir–Freundlich and Freundlich model could be respectively used to describe the two different adsorptions satisfactorily. Furthermore, the plane sheet diffusion model was successfully validated in this work. Diffusivities (D) of PED in CMCD-LDH film were determined from the homogeneous Fickian diffusion model. Compared with CMCD-LDH powder sample reported in our previous study, the structured CMCD-LDH film exhibits the advantages of more convenient operation and higher enantioselective adsorption ratio. It can be expected that this CMCD functionalized inorganic layered film may have potential application in the field of industrial chiral adsorption and separation.

Notation

a	thickness of the substrate, m
C	PED concentration in the CMCD-LDH film, mol/m^3
C_0	initial aqueous-phase PED concentration, mol/m^3
C_e	aqueous-phase PED concentration at equilibrium, mol/m^3
C_t	aqueous-phase PED concentration at time t, mol/m^3
D	diffusivity, m^2/s
F	fractional attainment of equilibrium
K	Freundlich temperature-dependent constant
K_L	Langmuir equilibrium constant, m^3/mol
l	the thickness of the film, m
m	the mass of CMCD-LDH, kg
Q_e	the adsorption capacity at equilibrium, mol/kg
Q_m	the Langmuir constant related to the capacity, mol/kg
$Q_{non-s,e}$	the non-enantioselective sorption capacity at equilibrium, mol/kg
$Q_{s,e}$	the enantioselective sorption capacity at equilibrium, mol/kg
Q_t	total PED amount in a film at time t, mol/kg
$Q_{total,e}$	the total sorption capacity at equilibrium, mol/kg
t	time, s
V	the volume of the solution, m^3
x	generic coordinate along the direction of diffusion, m

Acknowledgments

This project was supported by the National Natural Science Foundation of China, the Program for New Century Excellent Talents in University (Project no. NCET-05-121), the 973 Program (Grant no. 2009CB939802) and the Program for Changjiang Scholars and Innovative Research Team in University (Grant no. IRT0406).

References

Agrawal, A., Sahu, K.K., Pandey, B.D., 2004. A comparative adsorption study of copper on various industrial solid wastes. A.I.Ch.E. Journal 50, 2430–2438.

Chen, H.Y., Zhang, F.Z., Fu, S.S., Duan, X., 2006. In situ microstructure control of oriented layered double hydroxide monolayer films with curved hexagonal crystals as superhydrophobic materials. Advanced Materials 18, 3089–3093.

Choy, J.H., Kwak, S.Y., Jeong, Y.J., Park, J.S., 2000. Inorganic layered double hydroxides as nonviral vectors. Angewandte Chemie International Edition 39, 4041–4045.

Crank, J., 1975. The Mathematics of Diffusion. second ed. Oxford Science Publications, Oxford, UK.

Faucci, M.T., Melani, F., Mura, P., 2002. Computer-aided molecular modeling techniques for predicting the stability of drug—cyclodextrin inclusion complexes in aqueous solutions. Chemical Physics Letters 358, 383–390.

Gardner, E., Huntoon, K.M., Pinnavaia, T.J., 2001. Direct synthesis of alkoxide-intercalated derivatives of hydrocalcite-like layered double hydroxides: precursors for the formation of colloidal layered double hydroxide suspensions and transparent thin films. Advanced Materials 13, 1263–1266.

Gerardin, C., Kostadinova, D., Sanson, N., Coq, B., Tichit, D., 2005. Supported metal particles from LDH nanocomposite precursors: control of the metal particle size at increasing metal content. Chemistry of Materials 17, 6473–6478.

Giles, G.H., Mac Ewan, T.H., Nakhwa, S.N., Smith, P., 1960. Studies in adsorption: part XI. A system of classification of solution adsorption isotherms and its use in diagnosis of adsorption mechanisms and in measurement specific surface of solid. Journal of the Chemical Society 786, 3973–3993.

Gursky, J.A., Blough, S.D., Luna, C., Gomez, C., Luevano, A.N., Gardner, E.A., 2006. Particle–particle interactions between layered double hydroxide nanoparticles. Journal of the American Chemical Society 128, 8376–8377.

Hou, X.Q., Kirkpatrick, R.J., 2002. Interlayer structure and dynamics of ClO_4^- layered double hydroxides. Chemistry of Materials 14, 1195–1200.

Iwasaki, F., Maki, T., Nakashima, W., Onomura, O., Matsumura, Y., 1999. Nonenzymatic kinetic resolution of 1,2-diols catalyzed by an organotin compound. Organic Letters 1, 969–972.

Kijima, T., Matsui, Y., 1986. Preparation of modified cyclodextrins-pillared zirconium phosphate. Nature 322, 533–534.

Kijima, T., Tanaka, J., Matsui, Y., 1984. Synthesis of modified cyclodextrins-pillared montmorillonite. Nature 310, 45–47.

Lee, J.H., Rhee, S.W., Jung, D.Y., 2004. Solvothermal ion exchange of aliphatic dicarboxylates into the gallery space of layered double hydroxides immobilized on Si substrates. Chemistry of Materials 16, 3774–3779.

Lee, J.H., Rhee, S.W., Jung, D.Y., 2006. Ion-exchange reactions and photothermal patterning of monolayer assembled polyacrylate-layered double hydroxide nanocomposites on solid substrates. Chemistry of Materials 18, 4740–4746.

Li, L., Ma, R.Z., Ebina, Y., Fukuda, K., Takada, K., Sasaki, T., 2007. Layer-by-layer assembly and spontaneous flocculation of oppositely charged oxide and hydroxide nanosheets into inorganic sandwich layered materials. Journal of the American Chemical Society 129, 8000–8007.

Lipkowitz, K.B., Coner, R., Peterson, M.A., 1997. Locating regions of maximum chiral discrimination: a computational study of enantioselection on a popular chiral stationary phase used in chromatography. Journal of the American Chemical Society 119, 11269–11276.

Liu, X.L., Wei, M., Li, F., Duan, X., 2007. Intraparticle diffusion of 1-phenyl-1,2-ethanediol in layered double hydroxides. A.I.Ch.E. Journal 53, 1591–1600.

Liu, Z.P., Ma, R.Z., Osada, M., Iyi, N., Ebina, Y., Takada, K., Sasaki, T., 2006. Synthesis, anion exchange, and delamination of Co–Al layered double hydroxide: assembly of the exfoliated nanosheet/polyanion composite films and magneto-optical studies. Journal of the American Chemical Society 128, 4872–4880.

Lü, Z., Zhang, F.Z., Lei, X.D., Yang, L., Evans, D.G., Duan, X., 2007. Microstructure-controlled synthesis of oriented layered double hydroxide thin films: effect of varying the preparation conditions and a kinetic and mechanistic study of film formation. Chemical Engineering Science 62, 6069–6075.

Mohanambe, L., Vasudevan, S., 2005. Aromatic molecules in restricted geometries: photophysics of naphthalene included in a cyclodextrin functionalized layered solid. Journal of Physical Chemistry B 109, 22523–22529.

Nishi, H., Terabe, S., 1995. Optical resolution of drugs by capillary electrophoretic techniques. Journal of Chromatography A 694, 245–276.

Park, S.Y., Park, J.K., Park, J.H., McNeff, C.V., Carr, P.W., 2001. Separation of racemic 2,4-dinitrophenyl amino acids on carboxymethyl-β-cyclodextrin coated zirconia in RPLC. Microchemical Journal 70, 179–185.

Ravoo, B.J., Darcy, R., Mazzaglia, A., Nolan, D., Gaffney, K., 2001. Supramolecular tapes formed by a catanionic cyclodextrin in water. Chemical Communications, 827–828.

Rekharsky, M.V., Inoue, Y., 2002. Complexation and chiral recognition thermodynamics of 6-amino-6-deoxy-β-cyclodextrin with anionic, cationic, and neutral chiral guests: counterbalance between van der walls and coulombic interactions. Journal of the American Chemical Society 124, 813–826.

Sels, B.F., De Vos, D.E., Jacobs, P.A., 2005. Bromide-assisted oxidation of substituted phenols with hydrogen peroxide to the corresponding *p*-quinol and *p*-quinol ethers over WO_4^{2-}-exchanged layered double hydroxides. Angewandte Chemie International Edition 44, 310–313.

Sherma, J., 2002. Planar chromatography. Analytical Chemistry 74, 2653–2662.

Sips, R., 1948. On the structure of a catalyst surface. The Journal of Chemical Physics 16, 490–495.

Sun, P., Krishnan, A., Yadav, A., Singh, S., MacDonnell, F.M., Armstrong, D.W., 2007. Enantiomeric separations of ruthenium(II) polypyridyl complexes using high-performance liquid chromatography (HPLC) with cyclodextrin chiral stationary phases (CSPs). Inorganic Chemistry 46, 10312–10320.

Szejtli, J., 1998. Introduction and general overview of cyclodextrin chemistry. Chemical Reviews 98, 1743–1754.

Wang, J., Wei, M., Rao, G.Y., Evans, D.G., Duan, X., 2004. Structure and thermal decomposition of sulfated β-cyclodextrin intercalated in a layered double hydroxide. Journal of Solid State Chemistry 177, 366–371.

Wei, M., Zhang, X., Evans, D.G., Duan, X., Li, X.J., Chen, H., 2007. Rh-TPPTS intercalated layered double hydroxides as hydroformylation catalyst. A.I.Ch.E. Journal 53, 2916–2924.

Wei, M., Wang, J., He, J., Evans, D.G., Duan, X., 2005. In situ FT-IR, in situ HT-XRD and TPDE study of thermal decomposition of sulfated β-cyclodextrin intercalated in layered double hydroxides. Microporous and Mesoporous Materials 78, 53–61.

Williams, G.R., Dunbar, T.G., Beer, A.J., Fogg, A.M., O'Hare, D., 2006. Intercalation chemistry of the novel layered double hydroxides $[MAl_4(OH)_{12}](NO_3)_2 \cdot yH_2O$ (M = Zn, Cu, Ni and Co). 2: Selective intercalation chemistry. Journal of Materials Chemistry 16, 1231–1237.

Xiao, Y., Lim, H.M., Chung, T.S., Rajagopalan, R., 2007. Acetylation of β-cyclodextrin surface-functionalized cellulose dialysis membranes with enhanced chiral separation. Langmuir 23, 12990–12996.

Xu, Y.F., McCarroll, M.E., 2005. Fluorescence anisotropy as a method to examine the thermodynamics of enantioselectivity. Journal of Physical Chemistry B 109, 8144–8152.

Xu, Z.P., Braterman, P.S., 2007. Competitive intercalation of sulfonates into layered double hydroxides (LDHs): the key role of hydrophobic interactions. Journal of Physical Chemistry C 111, 4021–4026.

Zhao, H.T., Vance, G.F., 1997. Intercalation of carboxymethyl-β-cyclodextrin into magnesium–aluminum layered double hydroxide. Journal of the Chemical Society, Dalton Transactions, 1961–1965.

Zou, K., Zhang, H., Duan, X., 2007. Studies on the formation of 5-aminosalicylate intercalated Zn–Al layered double hydroxides as a function of Zn/Al molar ratios and synthesis routes. Chemical Engineering Science 62, 2022–2031.